Dual wavelength demultiplexing by coupling and decoupling of photonic crystal waveguides

F. S.-S. Chien

Center for Measurement Standards, 321 Kuang Fu Rd., Sect. 2, Hsinchu, Taiwan
forestchien@itri.org.tw

Y.-J. Hsu, W.-F. Hsieh

Department of Photonics Engineering, National Chiao Tung University, Hsinchu, Taiwan
wfhsieh@mail.nctu.edu.tw

S.-C. Cheng

Department of Physics, Chinese Culture University, Taipei, Taiwan
sccheng@faculty.pccu.edu.tw

Abstract: We demonstrate that the fundamental mode of the two coupled photonic crystal waveguides (PCWs) can be odd parity in a triangular photonic crystal and their dispersion curves do intersect. Thus, the PCWs are decoupled at the crossing point. By employing the decoupling at the crossing-point frequency and ultra short coupling length for another frequency, we designed a dual-wavelength demultiplexer with a coupling length of only two wavelengths and output power ratio as high as 15 dB. A loop-shape PCW is adapted to eliminate the backward energy flow.

OCIS codes: (060.4230) Multiplexing; (060.1810) Couplers, switches, and multiplexer; (130.2790) Guided waves; (130.3120) Integrated optics devices; (250.5300) Photonic integrated circuits; (230.7370) Waveguides.

References and links

1. E. Yablonovitch, "Inhibited spontaneous emission on solid-state physics and electronics," Phys. Rev. Lett. **58**, 2059-2062 (1987).
2. S. John, "Strong localization of photons on certain disordered dielectric superlattices," Phys. Rev. Lett. **58**, 2486-2488 (1987).
3. J. D. Joannopoulos, R. D. Meade and J. N. Winn, *Photonic Crystals—Molding the Flow of Light* (Princeton University Press, Princeton, 1995).
4. T. F. Krauss, and R. M. De La Rue, "Photonic crystals in the optical regime—past, present and future," Prog. Quantum Electron. **23**, 51-96 (1999).
5. R. D. Meade, A. Devenyi, J. D. Joannopoulos, O. L. Alerhand, D. A. Smith, and K. Kash, "Novel applications of photonic band gap materials: low-loss bends and high Q cavities," J. Appl. Phys. **75**, 4753-4755 (1994).
6. S. G. Johnson, P. R. Villeneuve, S. Fan, and J. D. Joannopoulos, "Linear waveguides on photonic-crystal slabs," Phys. Rev. B **62**, 8212-8222 (2000).
7. V. N. Astratov, R. M. Stevenson, I. S. Culshaw, D. M. Whittaker, M. S. Skolnick, T. F. Krauss and R. M. De La Rue, "Heavy photon dispersions in photonic crystal waveguides," Appl. Phys. Lett. **77**, 178-180 (2000).
8. M. Notomi, K. Yamada, A. Shinya, J. Takahashi, C. Takahashi, and I. Yokohama, "Extremely large group-velocity dispersion of line-defect waveguides in photonic crystal slabs," Phys. Rev. Lett. **87**, 253902-1 (2001).
9. A. Mekis, J. C. Chen, I Kurland, S. Fan, P. R. Villeneuve, and J. D. Joannopoulos, "High transmission through sharp bends in photonic crystal waveguides," Phys. Rev. Lett. **77**, 3787-3790 (1996).
10. S. Y. Lin, E. Chow, J. Bur, S. G. Johnson, and J. D. Joannopoulos, "Low-loss, wide-angle Y splitter at ~1.6-μm wavelengths built with a two-dimensional photonic crystal," Opt. Lett. **27**, 1400-1402 (2002).
11. M. Soljačić, S. G. Johnson, S. Fan, M. Ibanescu, E. Ippen, and J. D. Joannopoulos, "Photonic-crystal slow-light enhancement of nonlinear phase sensitivity," J. Opt. Soc. Am. B **19**, 2052-2059 (2002).

#3830 - $15.00 US Received 17 February 2004; revised 11 March 2004; accepted 14 March 2004

12. A. Martinez, A. Griol, P. Sanchis, and J. Marti, "Mach-Zehnder interferometer employing coupled-resonator optical waveguides," Opt. Lett. **28**, 405-407 (2003).
13. K. Hosomi, and T. Katsuyama, "A dispersion compensator using coupled defects in a photonic crystal," IEEE J. Quantum Electron. **38**, 825-829 (2002).
14. A. Martinez, F. Cuesta, and J. Marti, "Ultrashort 2-D photonic crystal directional couplers," IEEE Photon. Technol. Lett. **15**, 694-696 (2003).
15. A. Sharkawy, S. Shi, and D. W. Prather, "Electro-optical switching using coupled photonic crystal waveguides," Opt. Express **10**, 1048-1059 (2002).
16. M. Koshiba, "Wavelength division multiplexing and demultiplexing with photonic crystal waveguide couplers," J. Lightwave Technol. **19**, 1970-1975 (2001).
17. A. Sharkawy, S. Shi, and D. W. Prather, "Multichannel wavelength division multiplexing with photonic crystals," Appl. Optics **40**, 2247-2252 (2001).
18. S. Boscolo, M. Midrio, C. G. Someda, "Coupling and decoupling of electromagnetic waves in parallel 2-D photonic crystal waveguides," IEEE J. Quantum Electron. **38**, 47-53 (2002).
19. C. G. Someda, "Antiresonant decoupling of parallel dielectric waveguides," Opt. Lett. **16**, 1240-1242 (1991).
20. I. Vorobeichik, M. Orenstein, and N. Moiseyev, "Intermediate-mode-assisted optical directional couplers via embedded periodic structure," IEEE J. Quantum Electron. **34**, 1772-1781 (1998).
21. A. Taflove, *Computational Electrodynamics: The Finite-Difference Time-Domain Method* (Norwood, MA, Artech, 1995).
22. S. G. Johnson, and J. D. Joannopoulos, "Block-iterative frequency-domain methods for Maxwell's equations in a planewave basis," Opt. Express **8**, 173-190 (2001).
23. M. Bayindir, B. Temelkuran, and E. Ozbay, "Tight-binding description of the coupled defect modes in the three-dimensional photonic crystals," Phys. Rev. Lett. **84**, 2140-2143 (2000).
24. S. F. Mingaleev and Y. S. Kivshar, "Nonlinear transmission and light localization in photonic-crystal waveguides," J. Opt. Soc. Am. B **19**, 2241-2249 (2002).
25. S. Kuchinsky, V. Y. Golyatin, A. Y. Kutikov, T. P. Pearsall, D. Nedeljkovic, "Coupling between photonic crystal waveguides," IEEE J. Quantum. Electron. **38**, 1349-1352 (2002).

1. Introduction

Photonic crystals (PhCs) [1-4], composed of periodic dielectric materials, have been intensively studied in the past decade, because they possess many unique properties to control the propagation of electromagnetic (EM) waves. For instance, it has been demonstrated in PhCs the prohibition of propagating modes at certain frequency regions (the so-called photonic band gap), inhibition of spontaneous emission, and localization of EM waves in cavities. It may very well be possible to create large-scale photonic integrated circuits (PICs) based on PhCs and to improve the performance and cost efficiency of photonic systems. The photonic crystal waveguide (PCW) is one of the most promising elements of PhCs to be utilized in PICs [5,6]. A PCW is constructed by introducing a line defect into a perfect PhC to create defect modes within the photonic bandgap; thus, the EM wave propagating in the PCW is guided by the bandgap, instead of index-guided as in traditional waveguides. PCWs have various unmatched features such as extremely slow group velocity [7,8] and zero loss at sharp bends [9]. Many compact photonic devices based on PCWs have been proposed, e.g., splitters [10], Mach-Zehnder devices [11,12], and dispersion compensators [13].

Recently, the power transfer properties of parallel coupled PCWs have been studied, and devices such as directional couplers [14], switches [15], and multiplexers/demultiplexers, [16,17] have been proposed using the waveguide coupling. It is worth noting that the large dispersion of coupled mode splitting can be used to design various compact photonic devices. A special case is the extinction of power transfer (referred to as decoupling) resulting from the degeneracy of the eigenmodes [18]. The crosstalk between coupled PCWs is eliminated when the decoupling is present. High-density PICs can be easily achieved through the decoupling. For traditional waveguides, it is not an easy task to perform the decoupling [19,20]. It was claim in Ref. 18 that in two coupled PCWs, as long as a guiding structure is able to propagate only two modes, the electromagnetic component of the fundamental mode must always be of even parity. At no frequency can an odd mode become the fundamental mode. Hence, its dispersion curve can never cross that of the first even mode. Decoupling is impossible. In order to achieve decoupling or crossing dispersion, three defect modes are generated by

#3830 - $15.00 US Received 17 February 2004; revised 11 March 2004; accepted 14 March 2004

"adding new pillars at the center of the intra-core region" so that "the second and the third modes have opposite parities, and their dispersion relations intersect."

In this article, we found it is not always true that the fundamental mode must be of even parity. Without "adding new pillars at the center of the intra-core region" to generate "dispersion relations intersect", we do demonstrate the fundamental mode of the coupled PCWs can be odd parity in the triangular photonic crystal and the dispersion curves of the coupled PCWs intersect. Thus, the PCWs are decoupled at the crossing point. By employing the decoupling at the crossing-point frequency and ultra short coupling length for another frequency, we designed a dual-wavelength demultiplexer, which is a key component for the fiber-to-the-home optical network. The dispersive splitting and decoupling between coupled PCWs are described by the dispersion relations and verified by the finite-difference time-domain (FDTD) method [21]. The coupling region of the demultiplexer is only 5 lattice constants of the PhC, about two times as much as the wavelength interested. A loop layout of the output port is adapted to improve the output power ratios which show as high as 15 dB.

2. Coupling of PCWs

A two-dimensional (2D) PhC consists of a triangular lattice of dielectric rods with the lattice constant Λ in air. The diameter and the dielectric constant of the rods are 0.4 Λ and 12, respectively. To form a PCW a linear defect of void rods is introduced into the perfect PhC. The extended modes and the defect modes of the TM-polarization (the electric field parallels the rod axis) along the Γ-M direction are calculated by the plane wave expansion (PWE) method [22]. The bandgap ranges from the normalized frequency (f) 0.26 through 0.45 and the defect modes lie within the bandgap. The optical waves at defect modes are allowed to propagate within the PCW. The linear defect PCW can be regarded as a chain of point defects, and the defect mode is derived from the superposition of the longitudinal shifted eigenmodes of each individual point defect. The dispersion of a linear defect PCW is well fitted by

$$f = \Omega\,[1 + \kappa \cos(k_x \Lambda)], \tag{1}$$

from the tight-binding (TB) approximation [23,24], where Ω is the eigenfrequency of a single point defect and κ is the coupling coefficient. In Eq. (1), only the coupling of the nearest neighbor defects is taken into account.

As two parallel identical PCWs are brought close enough to have the defect modes well coupled, the defect modes will split into two eigenmodes. The smaller the separation of waveguides, the larger the coupling and the more splitting in dispersion of the eigenmodes.

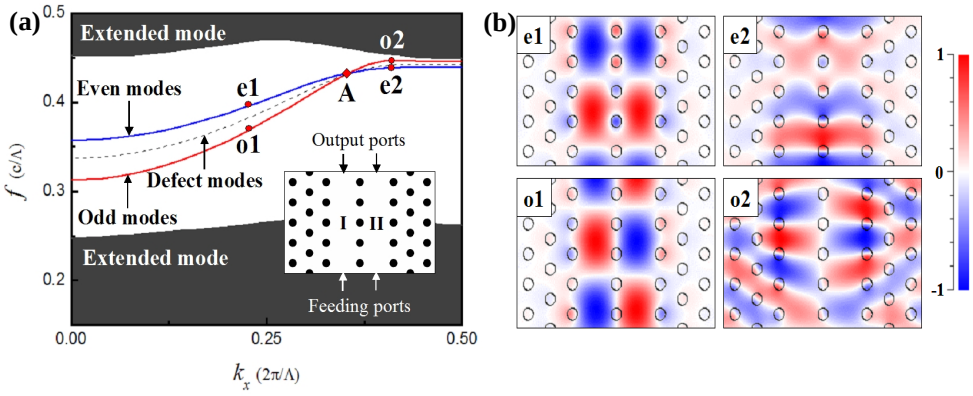

Fig. 1. (a) The energy band structures of the extended modes and defect modes of two coupled linear PCWs (I and II). The defect modes of the coupled PCWs are split into two eigenmodes, which cross at the point A. (b) The electric field patterns appear as even parity at the points of e1 and e2, and odd parity at o1 and o2. The poor confinement of the electric field at point o2 is a result of being close to the band edge.

#3830 - $15.00 US Received 17 February 2004; revised 11 March 2004; accepted 14 March 2004

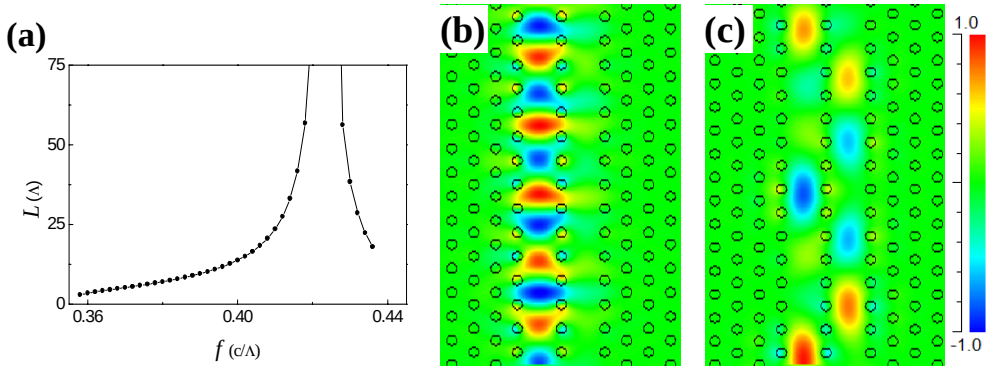

Fig. 2. (a) The plot of the coupling length L as the function of frequency. The L varies rapidly near f_A = 0.432 (L over 75 Λ is not shown). FDTD simulated electric field maps of the coupled PCWs at f_A (b) and f_B (= 0.361) (c) fed into PCW I. The coupling length of f_A is well beyond the simulated extent and that of f_B is 4.6 Λ. The field intensity in (c) decreases because part of the power flows backward, as discussed in Section 3.

Since a stronger coupling leads to a shorter coupling length, implying a shorter device, here we take the separation of two parallel PCWs (denoted as I and II) as 1 Λ. The dispersion relations are shown in Fig. 1(a). In addition, it is more convenient to proceed with the FDTD simulation of strong coupling since its simulated extent is smaller. From the mode patterns calculated by PWE, the eigenmodes appear to be an even parity and an odd parity (Fig. 1(b)). Unlike the traditional index-guiding waveguide, the odd mode mainly has an eigenfrequency lower than the even mode, since in this case the effective index of refraction at the guiding region of the PCW is lower than the index of the adjacent PhC. These two modes are degenerate at the point A (k_x = 0.353, f_A = 0.432). It has been reported that the coupling length L can be well described by the eigenmode expansion [18,25]; L can be written as $\Lambda/(2\Delta k)$, where $\Delta k = (k_1-k_2)$, and k_1 and k_2 are the normalized wavevectors of the even and odd modes at a given f. Apparently, Δk strongly depends on f, suggesting the splitting of large dispersion.

The analytic dispersion relations of even and odd modes can be separately obtained by fitting with Eq. (1), thus L as the function of f can be plotted as shown in Fig. 2(a). The value of L varies dramatically from 2.5 Λ to infinity for the coupled PCWs. Infinite L occurs at point A, attributed to the degeneracy of the eigenmodes and the fact that Δk = 0. Consequently, the incident optical wave excites either PCW I or II at f_A = 0.432, and is retained without crossing to the other PCW. The real-time evolution of the optical waves in the coupled PCWs is simulated by the FDTD method (Fig. 2(b)). If one launches a Gaussian wave with a width of $\sqrt{3}/2$ Λ at frequency f_A in the PCW I, then both eigenmodes will be excited. The optical wave keeps traveling in PCW I without observable power transferring into PCW II, even though its field extends over the PCW II. Hence, when they are operated at point A, the two PCWs are decoupled. Decoupling does not imply "no coupling" existing between the PCWs. In fact, those PCWs are still coupled at point A, but their two eigenmodes propagate at the same wavevector with no beating between the eigenmodes.

3. Demultiplexing

Let f_A correspond to λ_A = 1300 nm, and f_B = 0.361 for λ_B = 1550 nm thus L_B = 3.6 Λ and Δk = 0.136. The FDTD simulated optical wave of f_B transfers back and forth periodically between the two PCWs, because of beating of the eigenmodes (Fig. 2(c)). L is about 4.6 Λ close to the predicted value. The waves of f_A and f_B therefore would be demultiplexed, due to the distinction of decoupling and coupling. The demultiplexer of our preliminary design (denoted as Demux I) is shown in Fig. 3. Two feeding PCWs are separated by five rows of rods to prevent coupling, and the coupling region is 4 Λ long with one row separation. Clearly, the

#3830 - $15.00 US Received 17 February 2004; revised 11 March 2004; accepted 14 March 2004

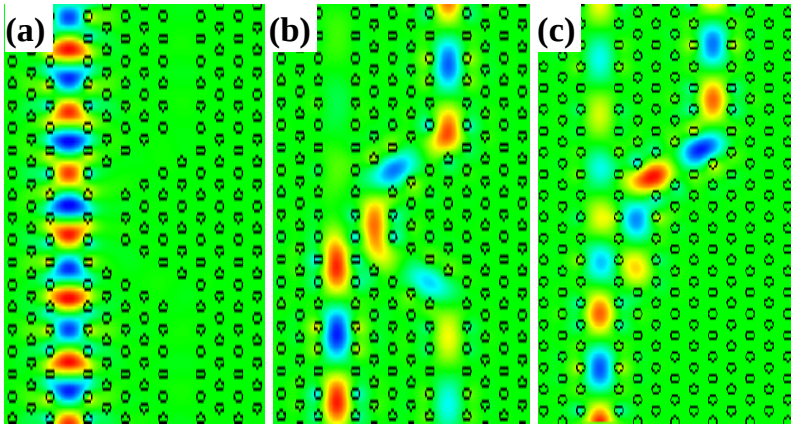

Fig. 3. FDTD simulated electric field maps of coupled PCWs; a bar state for f_A (a) and cross state for f_B (b), while both forward and backward couplings happen to f_B. As the feeding port of PCW II is removed (c), the wave of f_B transfers back to PCW I.

wave of f_A propagates only in PCW I without power transferring, and the wave of f_B completely transfers to the PCW II through the coupling region. In other word, the coupled PCWs demonstrate a bar state to f_A and a cross state to f_B. The output power ratio (the power at the desired output port to the residue power at the other output port, P_1/P_2) of f_A is 26 dB (Table 1). However, the ratio of f_B is only 10.7 dB, since the wave propagates in both forward and backward directions in PCW II. The efficiency of Demux I is reduced accordingly. The backward coupling is attributed to discontinuity of the effective index at the coupling region. To overcome this matter is not trivial, since various interactions, e.g., coupling, reflection, interference or diffraction, are present at the coupling region. As Fig. 3(c) shows, simply removing the feeding port of PCW II does not work, for the wave is bounced off the PCW II back to PCW I and the demultiplexing is destroyed.

Table 1. Output Power Ratios of Demultiplexers*

	Demux I		Demux II
	P_1/P_2 (dB)	P_1/P_3 (dB)	P_1/P_2 (dB)
f_A	26	26	15.6
f_B	10.7	6	16.2

* f_A= 0.432, f_B = 0.372. P_1 is the power at the desired output port, P_2 the residue power at the other output port, and P_3 the backward power of PCW II.

We therefore propose a novel design (denoted as Demux II) to deal with the backward coupling. Instead of removing the feeding port of PCW II, we make it a hexagonal loop with the coupling length of 5 Λ, as shown in Fig. 4. The backward coupled wave can merge with the forward wave after traveling the loop. In phase or constructive interference of the forward and backward waves at the merging point is crucial for maximum output power. If there is a phase mismatch, part of the coupled wave will transfer back to the PCW I. The interference can be tuned by changing the shape or size of the loop. The optimum design in Fig. 4(a) is to make the hexagonal loop three rows in width and five rows in length, so that the interference is constructive. The output power ratio of f_B is increased to 16.2 dB as the backward wave is eliminated (Table 1). The inevitable penalty is the output power ratio of f_A decreases to 15.6 dB, which is comparable to the previous result [14]. Some changes in either width or length of the loop will shift the constructive interference and decrease the output power ratio, as shown in Fig 4(b).

#3830 - $15.00 US Received 17 February 2004; revised 11 March 2004; accepted 14 March 2004

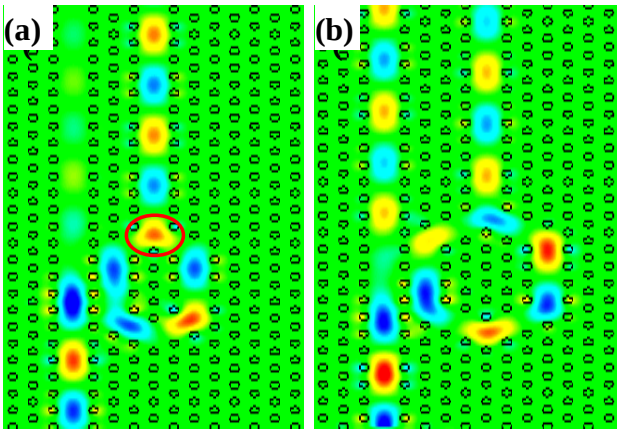

Fig. 4. (a) The loop layout applied to the PCW II for eliminating the backward coupling. The coupled forward and backward waves are in phase at the merging point (marked with the red circle). (b) The coupling efficiency decreases, as the waves are not in phase at the merging point. The frequency is f_B.

4. Discussion

For the extremely large splitting ($\Delta k = 0.136$) of the coupled PCWs, a coupling length of only 4.6 Λ is required for total transfer of power. In our design, the coupling region is 5 Λ (equal to two wavelengths). However, it is still rather tiny compared with traditional coupling devices of millimeter scale. In addition, only one L (for f_B) has to be taken into account for demultiplexing. That shortens the length required for power transfer and simplifies the design. The situation becomes more complicated if two different and finite Ls are involved at the coupling region.

We test the demultiplexing bandwidth by injecting an optical wave deviated from the nominal frequencies with the FDTD simulation. The available bandwidth ($\Delta f/f$) around f_B is about 5%. That is enough to cover the bandwidth of typical laser diodes employed in optical communication networks. The demultiplexer operated near f_A appears with a much wider bandwidth, because the coupling length is much longer than the coupling region. Hence the influence of coupling length variation can be ignored.

Here, we propose a novel design of the demultiplexer based on the unique properties of coupled PCWs and illustrate that the design is compact and practical, without yet pushing for its optimum performance. Overall, the dual wavelength demultiplexer is highly efficient and compact, and very useful to the high-density PICs. We believe the performance, for example, output power ratios, can be further improved by fine tune of the geometrical features. For instance, one can refine the design to have a coupling region with an integer multiple of the lattice constant to increase the output power ratios.

5. Conclusion

Without adding new rods at the center of the intra-waveguide region, we demonstrated the fundamental mode of the coupled PCWs can be odd parity in the triangular photonic crystal and the dispersion curves of the coupled PCWs do intersect. Thus, the PCWs are decoupled at the crossing point. By employing the decoupling at the crossing-point at wavelength of 1.3 μm and ultra short coupling length of 5 lattice constants at 1.55μm, we designed a dual-wavelength demultiplexer with output power ratio as high as 15 dB. A loop-shape PCW is proposed to increase the demultiplexing efficiency. A constructive interference at the merging point of the loop is necessary to have the maximum power transfer.

#3830 - $15.00 US Received 17 February 2004; revised 11 March 2004; accepted 14 March 2004

Acknowledgments

The authors would like to thank the National Center for High-performance Computing for the support of the FDTD simulation, the National Science Council and the Ministry of Economics of the Republic of China for partially financial support under grants NSC-92-2112-M-009-037 and 92C240.

#3830 - $15.00 US Received 17 February 2004; revised 11 March 2004; accepted 14 March 2004